

# Many-body localization transition in a frustrated XY chain

M. S. Bahovadinov,<sup>1,2</sup> D. V. Kurlov,<sup>1</sup> S. I. Matveenko,<sup>1,3</sup> B. L. Altshuler,<sup>4,1</sup> and G. V. Shlyapnikov<sup>1,5,6,7</sup>

<sup>1</sup>Russian Quantum Center, Skolkovo, Moscow 143025, Russia

<sup>2</sup>Physics Department, National Research University Higher School of Economics, Moscow, 101000, Russia\*

<sup>3</sup>L. D. Landau Institute for Theoretical Physics, Chernogolovka, Moscow region 142432, Russia

<sup>4</sup>Physics Department, Columbia University, 538 West 120th Street, New York, New York 10027, USA

<sup>5</sup>Moscow Institute of Physics and Technology, Inst. Lane 9, Dolgoprudny, Moscow Region 141701, Russia

<sup>6</sup>Université Paris-Saclay, CNRS, LPTMS, 91405 Orsay, France

<sup>7</sup>Van der Waals-Zeeman Institute, Institute of Physics, University of Amsterdam, Science Park 904, 1098 XH Amsterdam, The Netherlands

We study many-body localization (MBL) transition in a one-dimensional isotropic XY chain with a weak next-nearest-neighbor frustration in a random magnetic field. We perform finite-size exact diagonalization calculations of level-spacing statistics and fractal dimensions to demonstrate the MBL transition with increasing the random field amplitude. An equivalent representation of the model in terms of spinless fermions explains the presence of the delocalized phase by the appearance of an effective non-local interaction between the fermions. This interaction appears due to frustration provided by the next-nearest-neighbor hopping.

*Introduction.* The interplay of interparticle interactions and disorder in low-dimensional quantum systems is an old problem [1–4] and it has been an active research direction in the recent years. Numerous numerical studies of disordered interacting one-dimensional (1D) quantum systems suggest a transition to the many-body localized (MBL) phase, when the amplitude of diagonal disorder is sufficiently large. In the MBL phase the eigenstate thermalization hypothesis (ETH) is violated [5–10], which implies protection of quantum states from decoherence and opens new prospects for quantum information storage. Recent numerical studies of the MBL phase also show unusual entanglement properties [11–14] and vanishing steady transport [15–18]. Some of these properties can be explained in terms of emerging quasi-local integrals of motion [19–21]. The MBL transition is usually characterized by the level-spacing statistics [22–27], participation entropies [28, 29], underlying entanglement structure of eigenstates [13, 26, 30], and by quantum correlations of neighboring states [23, 31].

The Heisenberg spin-1/2 chain in a random magnetic field has been considered as a toy model for almost all numerical studies of the MBL transition [22–24]. Special attention should be paid to promising theoretical models, which can be realized experimentally using ultra-cold atoms, trapped ions, and superconducting circuits. Studying the MBL transition for trapped ions or polar molecules one should take into account long-range interaction (LRI) and hopping (LRH) terms, which are naturally present in these systems. The consideration of LRH terms has started with the seminal work of Anderson on disordered  $d$ -dimensional non-interacting fermionic systems with  $J_{ij} \sim r_{ij}^{-\alpha}$  ( $J_{ij}$  and  $r_{ij}$  are the hopping amplitude and distance between the  $i$ -th and  $j$ -th sites, re-

spectively). It predicts delocalization for  $\alpha \leq d$  at any disorder strength even at  $T = 0$  [32]. A natural extension of this study to many-body quantum systems with the Ising-type LRI  $V_{ij} \sim r_{ij}^{-\alpha} S_i^z S_j^z$  ( $S_i^z$  is the  $z$ -component of the spin operator of a particle), modifies the above criterion to  $\alpha < 2d$  [33, 34], implying a possibility of the MBL transition for  $\alpha > 2d$ .

LRH (*flip-flop* hoppings) quantum spin models without explicit diagonal interaction terms also exhibit the MBL transition in the presence of the on-site diagonal disorder. This scenario was studied for  $d$ -dimensional XY magnets with  $J_{ij} \sim r_{ij}^{-\alpha}$  in a random transverse magnetic field [35]. It was shown that being explicitly absent initially, the Ising-type interaction is generated in the third order of perturbation theory in hopping [35]. This interaction delocalizes states for  $\alpha > 3d/2$  provided that the disorder is sufficiently weak. In contrast to this result, numerical studies based on exact diagonalization (ED) and matrix product states indicate the MBL transition for  $\alpha \geq 1$  in 1D systems [36, 37].

Experimentally, the 1D LRH XY chain was recently realized using trapped  $\text{Ca}^+$  ions ( $\alpha < 3$ ) and using this setup a new protocol of measuring entanglement entropy was demonstrated [38]. On the other hand, recent proposal [39] suggests realization of the 1D XY model using superconducting arrays of three-dimensional transmons with interqubit dipolar interactions. In the proposed model only the nearest-neighbor and next-nearest-neighbor hoppings are present, whereas other hopping terms exactly vanish. It is reasonable to analyse the interplay between the frustration natural to LRH XY magnets, and the diagonal disorder in this simplified model.

In the present paper we show the existence of the many-body localization - delocalization transition in the latter model. We demonstrate that the presence of the next-nearest-neighbor hopping, which provides the frustration, is crucial for the MBL transition. This

\* mbahovadinov@hse.ru

is revealed by using the Jordan-Wigner transformation, which maps the original spin model onto the model of spinless fermions. The fermionic model consists of hopping terms to the two nearest sites and a non-local interaction term. In the absence of frustration in the original spin model, the non-local interaction and next-nearest-neighbor hopping terms vanish and we have the system of free fermions where the states are known to be localized in arbitrarily weak potential disorder.

*Model and methods.* We consider a one-dimensional frustrated spin-1/2 isotropic  $XY$  spin chain [40] in a random magnetic field. The Hamiltonian of the system has the following form:

$$H = \sum_{\beta=1,2} J_{\beta} \sum_{j=1}^L \left[ S_j^x S_{j+\beta}^x + S_j^y S_{j+\beta}^y \right] + \sum_{j=1}^L h_j S_j^z, \quad (1)$$

where  $J_{1,2} > 0$  are exchange interaction coupling constants, and  $h_j$  are uncorrelated random field amplitudes from the uniform distribution  $[-h, h]$ . We consider the problem in the ring geometry with (even)  $L$  sites. In the absence of disorder the Hamiltonian (1) is translationally invariant and possesses the  $U(1)$  and parity symmetries [41], and all these symmetries are broken in the presence of disorder. However, if either  $J_1 = 0$  or  $J_2 = 0$ , the Hamiltonian (1) is integrable for arbitrary  $h_j$  since in this case it can be mapped onto the system of free fermions. Also, if  $h_j = 0$  and  $\kappa = J_2/J_1 \ll 1$  the model (1) can be shown to be *quasi-integrable* [42], similarly to the Heisenberg model weakly perturbed by the next-nearest neighbor isotropic interactions [50].

The low-temperature phase diagram of the clean model (1) was earlier studied extensively using numerical techniques such as density matrix renormalization group (DMRG) and ED methods [51, 52]. It is known that for  $\kappa \lesssim 0.32$  the system is in the gapless Tomonaga-Luttinger liquid phase, where expectation values of spin operators vanish and two-point correlation functions exhibit power-law decay. For  $\kappa \gtrsim 0.32$  the gapped insulating phase (singlet dimer phase) is developed via the Berezinskii-Kosterlitz-Thouless-type transition. In the limits of  $\kappa = 0$  and  $\kappa = \infty$  the clean model (1) is integrable. In the former case, the unfrustrated  $XY$  chain is restored, while the second case corresponds to two decoupled  $XY$  chains. We hereafter restrict our consideration with  $\kappa < 0.32$ , so that the ground state is in the gapless phase.

*Characterization of eigenstates.* An important quantity that characterizes the eigenstates of the disordered model is the ratio of the minimum to maximum level spacing,

$$r_i = \frac{\min(\Delta_i, \Delta_{i+1})}{\max(\Delta_i, \Delta_{i+1})}, \quad \Delta_i = \epsilon_i - \epsilon_{i-1}, \quad (2)$$

where  $\epsilon_i$  are the ordered energy eigenvalues for a given realization of disorder. In the delocalized (chaotic) phase

the energy level spacing distribution obeys Wigner's surmise of Gaussian orthogonal ensemble (GOE), while in the localized phase no level repulsion is expected and there is a Poissonian distribution (PS) of the level spacings. For the PS distribution the disorder-averaged value is  $\langle r \rangle_P = 2 \ln 2 - 1 \approx 0.386$ , and for the Wigner-Dyson (WD) distribution one has  $\langle r \rangle_W = 0.5307(1)$  [24].

We next consider localization of eigenstates in the Hilbert space. For the model (1) with  $L$  sites and a fixed total magnetization  $S^z$  one has  $\mathcal{N}_{\mathcal{H}}$ -dimensional Hilbert space, with  $\mathcal{N}_{\mathcal{H}} < 2^L$ . We analyze many-body eigenstates in the computational basis  $|s\rangle = |s_1\rangle \otimes |s_2\rangle \otimes \dots \otimes |s_L\rangle$ , with local states  $|s_i\rangle \in \{|\uparrow\rangle, |\downarrow\rangle\}$ . The quantities well characterizing localization properties of the wavefunctions  $\psi_{\alpha}(s) = \langle s|\alpha\rangle$  are the fractal dimensions  $D_q$ . The set of  $D_q$  is determined from the scaling of participation entropies  $S_q$  with  $\mathcal{N}_{\mathcal{H}}$ ,

$$S_q = \frac{1}{q-1} \ln \left( \sum_{s=1}^{\mathcal{N}_{\mathcal{H}}} |\psi_{\alpha}(s)|^{2q} \right) \xrightarrow{\mathcal{N}_{\mathcal{H}} \rightarrow \infty} D_q \ln(\mathcal{N}_{\mathcal{H}}). \quad (3)$$

Eigenstates  $|\alpha\rangle$  localized (LO) on a finite set of  $|s\rangle$  have  $S_q$  independent of  $\mathcal{N}_{\mathcal{H}}$  and thus  $D_q = 0$  for any  $q > 0$ . On the other hand, extended ergodic (EE) states with  $|\psi_{\alpha}(s)|^2 \sim \mathcal{N}_{\mathcal{H}}^{-1}$  give  $D_q = 1$ . The multifractal states with  $0 < D_q < 1$  are non-ergodic albeit extended (NEE). We confine ourselves to the *Shannon limit* ( $q \rightarrow 1$ ) in Eq. (3).

The MBL transition can be equally identified via characterization of quantum correlations between neighboring (in energy) eigenstates. The corresponding quantity is the Kullback-Leibler divergence  $KL$  [53–55]:

$$KL = \sum_{s=1}^{\mathcal{N}_{\mathcal{H}}} |\psi_{\alpha}(s)|^2 \ln \left( \frac{|\psi_{\alpha}(s)|^2}{|\psi_{\alpha+1}(s)|^2} \right), \quad (4)$$

where the states  $|\alpha\rangle$  are supposed to be ordered in energy. The NEE states close to this transition can be viewed as the result of the hybridization of LO states. The LO states are not correlated in space and the ratio  $|\frac{\psi_{\alpha}(s)}{\psi_{\alpha+1}(s)}|$  is exponentially large if  $|\psi_{\alpha}(s)|$  is not negligible, i.e.  $KL \rightarrow \infty$  for  $\mathcal{N}_{\mathcal{H}} \rightarrow \infty$ . After the hybridization, NEE states  $|\alpha\rangle$  and  $|\alpha+1\rangle$  involve mostly the same LO states. As a result  $|\psi_{\alpha}(s)|$  and  $|\psi_{\alpha+1}(s)|$  are strongly correlated with  $|\frac{\psi_{\alpha}(s)}{\psi_{\alpha+1}(s)}| \sim O(1)$  and  $KL$  is finite. An abrupt change of  $KL$  is therefore an indication of the MBL transition.

We study the MBL transition for eigenstates with energies close to zero (eigenstates from the central part of the spectrum), although this transition can be observed at any energy density (assuming sufficiently strong frustration to delocalize low-energy eigenstates). For lattice sizes  $L = \{14, 16, 18, 20\}$  we employ the shift-invert ED algorithm based on  $LDL^T$  decomposition to obtain  $m = \{20, 20, 40, 100\}$  eigenstates. We consider the problem in the largest Hilbert subspace (at total magnetization  $S^z = 0$ ) with dimensions  $\mathcal{N}_{\mathcal{H}} = \binom{L}{L/2}$ . We note

that the MBL transition in the other sectors is non-trivial due to the non-local nature of emergent interaction. The number of disorder realizations for a given disorder strength  $h$  varies from  $10^4$  for the smallest lattice size up to  $10^2$  for the largest size. We average quantities of our interest over the  $m$  states and then the disorder averaging is performed.

*Jordan-Wigner fermionization.* Before turning to our numerical results we point out that there is an implicit interaction which induces delocalization. Naively, one may expect that spin fluctuations in our model should be localized by disorder like fermionic fluctuations, and the states should undergo AL in arbitrarily weak random magnetic fields. We show here that this is not the case. This is due to the statistics of spins which has neither pure bosonic nor pure fermionic character. However, one may fully fermionize the spin problem by using the Jordan-Wigner (JW) transformation [56]:

$$S_i^+ = c_i^\dagger e^{i\pi \sum_{p < i} \hat{n}_p}, \quad S_i^z = \hat{n}_i - 1/2, \quad (5)$$

where  $\hat{n}_i = c_i^\dagger c_i$  and the operators  $c_i^\dagger, c_i$  obey the canonical fermionic anti-commutation relations. From Eq. (5) one immediately sees that  $S_i^+ S_j^- = c_i^\dagger \hat{\Phi}_{i,j} c_j$ , where the Hermitian operator  $\hat{\Phi}_{i,j}$  is given by

$$\hat{\Phi}_{i,j} = \prod_{l=i+1}^{j-1} (1 - 2\hat{n}_l), \quad j \geq i + 2, \quad (6)$$

and reduces to  $\hat{\Phi}_{i,j} = 1$  for  $j = i + 1$ . Then, applying the JW transformation to Eq. (1) we obtain :

$$H^F = \sum_{\beta=1,2} \frac{J_\beta}{2} \sum_{i=1}^L \left( c_i^\dagger c_{i+\beta} + \text{H.c.} \right) + V_{\text{int}} + \sum_i h_i \hat{n}_i, \quad (7)$$

with the non-local interaction (correlated hopping) term

$$V_{\text{int}} = -J_2 \sum_{i=1}^L \left( c_i^\dagger \hat{n}_{i+1} c_{i+2} + \text{H.c.} \right). \quad (8)$$

We thus have an interacting fermionic system with a non-local interaction in a potential disorder. In the absence of frustration (i.e. for  $J_2 = 0$ ) the interaction and next-nearest-neighbor hopping are equal to zero, and in Eq. (7) one has a system of free fermions with nearest-neighbor hopping in the potential disorder, where all states are localized. It is the non-local interaction  $V_{\text{int}}$  that can lead to delocalization, as we show below. This becomes clear if one replaces the first term in the Hamiltonian (1) for  $\beta = 2$  with  $J_2 \sum_i (S_i^x S_{i+2}^x + S_i^y S_{i+2}^y) S_{i+1}^z$ . We then arrive at the so-called XZX+YZY model which maps onto the free-fermionic limit of Eq. (7) [57], where  $V_{\text{int}} = 0$  but there is the next-nearest-neighbor hopping on top of the nearest neighbor one. The states in this case are localized in a weak disorder [32] (see Fig. 1).

While the fermionic correlated hopping term (8) is hard to analyse, simple qualitative explanation can be given using alternative representation of the clean model (1) in terms of hard-core bosons,

$$H^B = \sum_{i,\beta} \frac{J_\beta}{2} (b_i^\dagger b_{i+\beta} + \text{H.c.}) \quad (9)$$

When  $J_1 = 0$  or  $J_2 = 0$ , hard-core bosons hop around the ring, while strictly keeping their ordering, i.e no particle exchange occurs. This implies that the statistics of bosons is not exhibited in this case due to the imposed hard-core constraint on bosons. In fact, it is this ordering which guarantees JW mapping onto free spinless fermions, where the hard-core constraint plays a role of Pauli principle. However, this single-particle behavior does not hold when additional hopping channel is introduced and particle exchange is no longer prohibited. At  $T = 0$  hard-core bosons start to form off-diagonal quasi-long-range order and exhibit *algebraic superfluidity*. Furthermore, hard-core interaction does not allow more than one particles in a given site and this requires critical disorder strength to localize states, implying superfluid-Bose glass transition [58, 59].

We lastly note that the long-range hopping limit of Eq. (1) fermionizes with many-body interacting terms encapsulated in the JW phase Eq. (6). In general, the hopping to the  $\beta$  nearest sites generates up to  $\beta$ -body interaction. This can be seen already in the  $\beta = 3$  case:

$$H_3^I \mapsto J_3 c_i^\dagger (\hat{1} - 2\hat{n}_{i+1} - 2\hat{n}_{i+2} + 4\hat{n}_{i+1}\hat{n}_{i+2}) c_{i+3}. \quad (10)$$

Here, the first term corresponds to the fermionic hopping, while the other terms generate many-body interactions. Thus, one has to take into account this type of interaction terms in the studies of frustrated spin models [60].

*Numerical ED results.* In this section we present our numerical results for  $\kappa = 0.1$ , which demonstrate the MBL transition when the strength of the random magnetic field exceeds a critical value. We identify the MBL transition exploiting the average gap ratio for adjacent eigenstates  $\langle r \rangle$ , defined in Eq. (2). Our findings are illustrated in Fig. 1(a).

For the disorder strength  $h/J_1 \lesssim 1$  the energy mini-gaps obey the WD statistics with  $\langle r \rangle_{\text{W}} \approx 0.53$ . This implies the presence of hybridization between regions of the system that are long-distant from each other, which results in the level repulsion between the neighboring eigenstates. For all system sizes that we consider the benchmarked WD level  $\langle r \rangle_{\text{W}}$  is observed in a finite interval of  $h/J_1$ , although for our smallest system size  $L = 14$  the finite-size effects are the strongest and the WD distribution is not fully obeyed. When the disorder strength is further increased, the energy mini-gap statistics deviates from the WD distribution but does not yet acquire the full PS character. The curves corresponding to different  $L$  in Fig. 1 cross each other in the vicinity of the

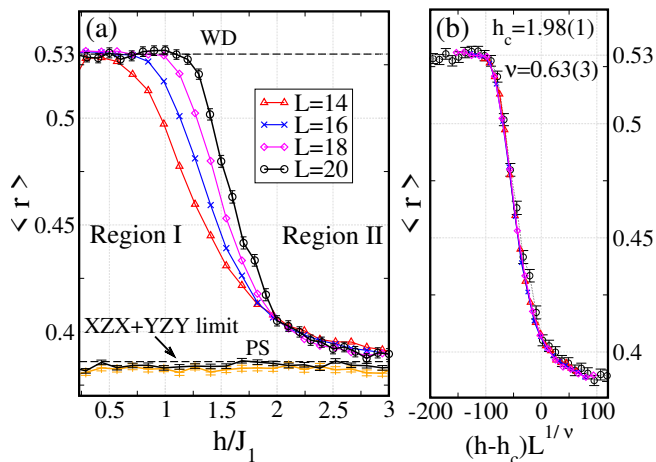


FIG. 1. (a) Dependence of the average gap ratio  $\langle r \rangle$  on the disorder strength  $h$  for the system sizes  $L = \{14, 16, 18, 20\}$  at  $\kappa = 0.1$ . The MBL phase (Region II) is separated from the delocalized phase (Region I) at the  $h_c/J_1 \approx 1.98$ . In the XZX+YZY limit the states are localized and  $\langle r \rangle = \langle r \rangle_P \approx 0.386$  for all disorder amplitudes. (b) Implementation of the scaling ansatz leads to the collapse of numerical data to a single universal curve with  $h_c/J_1 = 1.98 \pm 0.01$  and  $\nu = 0.63 \pm 0.03$ .

critical point  $h/J_1 \approx 2$ . When the system size is further increased the crossing points drift to larger values of disorder strength and in the thermodynamic limit the convergence of the crossing points to the critical point is expected. Using the finite-size calculation results, the behavior of  $\langle r \rangle$  near the critical point can be analyzed via the scaling form  $\langle r \rangle \sim f(L^{1/\nu}(h - h_c))$ , with the scaling function  $f$  [23]. Direct implementation of this scaling ansatz leads to the collapse of all data to a single universal curve (see Fig. 1(b)) with  $h_c/J_1 = 1.98 \pm 0.01$  and  $\nu = 0.63 \pm 0.03$  [61]. For the disorder strength  $h > h_c$  the states are in the MBL phase and the gap statistics converges to the PS distribution with  $\langle r \rangle_P \approx 0.39$ .

The character of the demonstrated MBL transition is similar to the one for the 1D Heisenberg chain in a random magnetic field [23, 24]. The stabilization of the delocalized phase in the latter case is guaranteed by the Ising interaction term ( $\hat{n}_i \hat{n}_{i+1}$  for fermions), whereas in our model it occurs due to the interaction term  $V_{\text{int}}$ . To finalize this argument, we repeated our calculations of  $\langle r \rangle$  for the system sizes  $L = \{16, 18\}$  when the interaction term is removed (XZX+YZY limit). The corresponding plots are presented in Fig. 1(a). For both considered system sizes a stable PS distribution of level spacings with  $\langle r \rangle = \langle r \rangle_P \approx 0.39$  is exhibited, which corresponds to full (Anderson) localization of eigenstates.

The MBL transition is also correctly captured by the fractal dimensions presented in Fig. 2. In the delocalized phase the support set of states covers a sufficiently large fraction of the Hilbert space with  $|\psi(j)|^2 \sim \mathcal{N}_{\mathcal{H}}^{-1}$  in the thermodynamic limit. This implies  $D_q \rightarrow 1$ ,

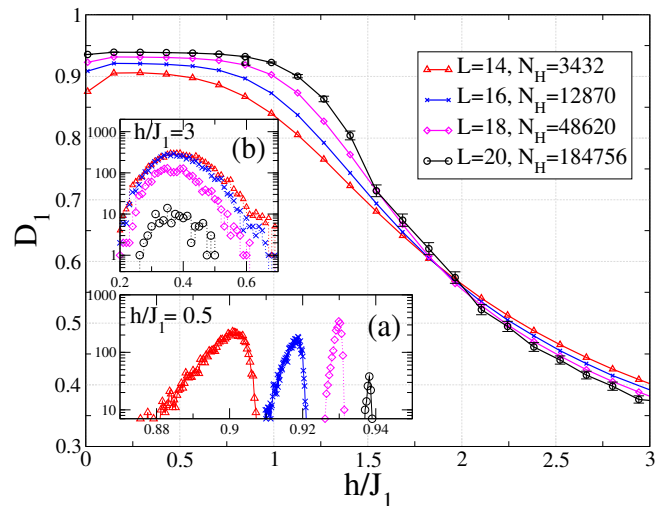


FIG. 2. Fractal dimensions  $D_1$  versus the disorder strength  $h/J_1$  for  $L = \{14, 16, 18, 20\}$ . Insets show scaled histograms  $P(D_1)$  for two representative disorder amplitudes (a) at the delocalized phase ( $h/J_1 = 0.5$ ) and (b) at the MBL phase ( $h/J_1 = 3$ ). Error bars smaller than the symbol size are omitted.

$S_q \sim \ln(\mathcal{N}_{\mathcal{H}})$  as  $\mathcal{N}_{\mathcal{H}} \rightarrow \infty$ . In our finite-size calculations  $D_1$  is practically independent of  $h/J_1$  in a finite interval of  $h/J_1$  with the values  $D_1 = \{0.900, 0.922, 0.931, 0.939\}$  for the system sizes  $L = \{14, 16, 18, 20\}$ , respectively. The convergence of  $D_1$  towards unity with increasing the system size is demonstrated clearly by the histograms with a vanishing variance Fig. 2(a). In the thermodynamic limit the constant value  $D_1 = 1$  is expected within the delocalized phase, with an abrupt jump to  $D_1 = 0$  at the critical field. In the MBL phase the distribution of  $D_1$  has an opposite skewness and converges towards zero with growing the system size as shown in Fig. 2(b). As expected, the benchmarked critical point lies within the transition area determined from  $D_1$  curve-crossings.

Strong quantum correlations between nearby eigenstates in the chaotic regime result in the known value of  $KL_{\text{GOE}} = 2$ , which is demonstrated in Fig. 3 (left). This value is kept within the delocalized region, which widens with increasing the system size. On the other hand, neighboring eigenstates in the MBL phase are weakly correlated and this results in the divergent behavior  $KL \sim \ln(\mathcal{N}_{\mathcal{H}})$ . These distinctive features are also demonstrated in the scaled histogram plots in the insets of Fig. 3. In the delocalized phase [Fig. 3 (a)] the distribution of  $KL$  has a Gaussian form with the mean value  $KL \approx 2$  and the variance vanishing with increasing  $L$ . On the contrary, in the MBL phase the situation is different and both the mean value and the variance increase with  $L$  [Fig. 3 (b)]. Although a large drift of crossing points with increasing the system size does not allow one to do a precise finite-size scaling analysis, it is clear that the crossing point of the last two curves

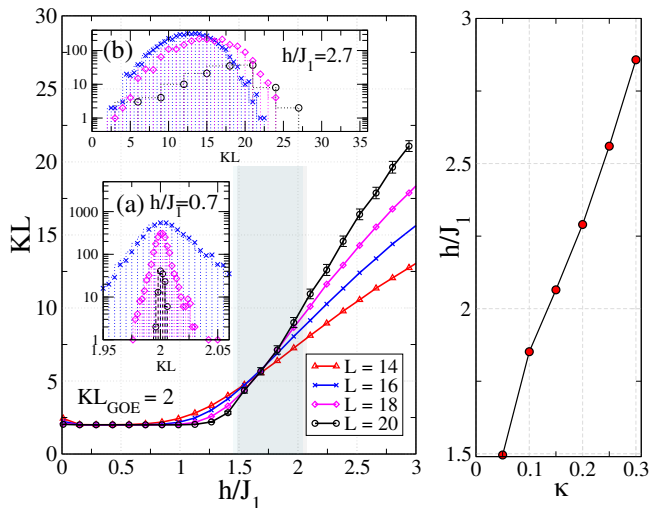


FIG. 3. Kullback-Leibler divergence  $KL$  as a function of disorder strength  $h/J_1$  for  $L = \{14, 16, 18, 20\}$  (left) and finite-size phase boundary in the  $\kappa - h$  space (right). Insets show scaled histograms  $P(KL)$  (a) at the MBL phase ( $h/J_1 = 2.7$ ) and (b) at the delocalized phase ( $h/J_1 = 0.7$ ).

(corresponding to the largest Hilbert spaces) lies in the critical region determined above and it is close to the benchmarked critical field.

We then performed ED calculations of  $D_1$  for other values of  $\kappa = J_2/J_1 \lesssim 0.32$ , such that the ground state is still in the gapless phase. The determined finite-size critical field strengths  $h_c(\kappa)/J_1$  based on curve-crossings of  $D_1$  (corresponding to  $L = 14$  and  $L = 16$ ) are presented in Fig. 3 (right). The provided figure is far from serving as a phase diagram in the  $\kappa - h$  space. However, it qualitatively demonstrates that an increase of  $\kappa$  should increase the interaction strength in Eq.(8) and, hence, should lead to the enhancement of the delocalization effect of the frustration. This indeed results in a linear growth of  $h_c/J_1$  with  $\kappa$ , as shown in Fig. 3 (right). In the limit of  $\kappa \rightarrow \infty$  we arrive at two weakly coupled XY chains and the critical field should decrease, reaching  $h_c = 0$  at  $\kappa = \infty$ .

*Conclusions.* We have demonstrated the MBL transition in a 1D weakly frustrated XY magnet in a random magnetic field using analytical arguments and numerical ED calculations. We exploited the Jordan-Wigner transformation to map the spin model onto the system of interacting fermions with a non-local interaction. This interaction originates from the presence of frustration and is responsible for the emergence of delocalization in a random magnetic field. Our results for the level-spacing statistics show the presence of quantum correlations between the neighboring eigenstates and the resulting level repulsion in the delocalized phase. In the limit of strong disorder, the neighboring eigenstates are weakly hybridized and the system is in the MBL phase. This leads to the vanishing level repulsion, and energy mini-

gaps obey the PS statistics. These results are supported by the calculation of fractal dimensions and characterization of quantum correlations of neighboring eigenstates.

In summary, our results demonstrate an important role of frustration hopping terms in disordered spin models. The discussed effect can be generalized to other quasi-1D geometries, where the JW phase survives. Experimentally, the discussed MBL transition can be realized, e.g., by using a setup of superconducting qubit arrays proposed in Ref. [39].

We thank V. Gritsev and W. Buijsman for useful comments and discussions. This research was supported in part through computational resources of HPC facilities at HSE University [62] and by the Russian Science Foundation Grant No. 20-42-05002. We also acknowledge support of this work by Rosatom.

- 
- [1] W. Apel and T. M. Rice, *J. Phys. C: Solid State Phys.* **16**, L271 (1983).
  - [2] T. Giamarchi and H. J. Schulz, *Phys. Rev. B* **37**, 325 (1988).
  - [3] D. Basko, I. Aleiner, and B. Altshuler, *Ann. Phys.* **321**, 1126 (2006).
  - [4] I. V. Gornyi, A. D. Mirlin, and D. G. Polyakov, *Phys. Rev. Lett.* **95**, 206603 (2005).
  - [5] A. Pal and D. A. Huse, *Phys. Rev. B* **82**, 174411 (2010).
  - [6] Y. Bar Lev and D. R. Reichman, *Phys. Rev. B* **89**, 220201 (2014).
  - [7] M. Serbyn, Z. Papić, and D. A. Abanin, *Phys. Rev. X* **5**, 041047 (2015).
  - [8] D. J. Luitz, N. Laflorencie, and F. Alet, *Phys. Rev. B* **93**, 060201 (2016).
  - [9] A. De Luca and A. Scardicchio, *Europhys. Lett.* **101**, 37003 (2013).
  - [10] A. De Luca, B. L. Altshuler, V. E. Kravtsov, and A. Scardicchio, *Phys. Rev. Lett.* **113**, 046806 (2014).
  - [11] B. Bauer and C. Nayak, *J. Stat. Mech.* **2013**, P09005 (2013).
  - [12] M. Serbyn, Z. Papić, and D. A. Abanin, *Phys. Rev. Lett.* **110**, 260601 (2013).
  - [13] W. Buijsman, V. Gritsev, and V. Cheianov, *Phys. Rev. B* **100**, 205110 (2019).
  - [14] M. Serbyn, A. A. Michailidis, D. A. Abanin, and Z. Papić, *Phys. Rev. Lett.* **117**, 160601 (2016).
  - [15] T. C. Berkelbach and D. R. Reichman, *Phys. Rev. B* **81**, 224429 (2010).
  - [16] O. S. Barišić, J. Kokalj, I. Balog, and P. Prelovšek, *Phys. Rev. B* **94**, 045126 (2016).
  - [17] Y. Bar Lev, G. Cohen, and D. R. Reichman, *Phys. Rev. Lett.* **114**, 100601 (2015).
  - [18] P. Prelovšek and J. Herbrych, *Phys. Rev. B* **96**, 035130 (2017).
  - [19] M. Serbyn, Z. Papić, and D. A. Abanin, *Phys. Rev. Lett.* **111**, 127201 (2013).
  - [20] L. Rademaker and M. Ortuño, *Phys. Rev. Lett.* **116**, 010404 (2016).
  - [21] A. Chandran, I. H. Kim, G. Vidal, and D. A. Abanin, *Phys. Rev. B* **91**, 085425 (2015).

- [22] K. Kudo and T. Deguchi, *Phys. Rev. B* **97**, 220201 (2018).
- [23] D. J. Luitz, N. Laflorencie, and F. Alet, *Phys. Rev. B* **91**, 081103 (2015).
- [24] V. Oganesyan and D. A. Huse, *Phys. Rev. B* **75**, 155111 (2007).
- [25] C. L. Bertrand and A. M. García-García, *Phys. Rev. B* **94**, 144201 (2016).
- [26] V. Khemani, S. P. Lim, D. N. Sheng, and D. A. Huse, *Phys. Rev. X* **7**, 021013 (2017).
- [27] V. Khemani, D. N. Sheng, and D. A. Huse, *Phys. Rev. Lett.* **119**, 075702 (2017).
- [28] N. Maće, F. Alet, and N. Laflorencie, *Phys. Rev. Lett.* **123**, 180601 (2019).
- [29] E. J. Torres-Herrera and L. F. Santos, *Phys. Rev. B* **92**, 014208 (2015).
- [30] J. Gray, S. Bose, and A. Bayat, *Phys. Rev. B* **97**, 201105 (2018).
- [31] M. Pino, J. Tabanera, and P. Serna, *J. Phys. A: Math. Theor.* **52**, 475101 (2019).
- [32] P. W. Anderson, *Phys. Rev.* **109**, 1492 (1958).
- [33] N. Y. Yao, C. R. Laumann, S. Gopalakrishnan, M. Knap, M. Müller, E. A. Demler, and M. D. Lukin, *Phys. Rev. Lett.* **113**, 243002 (2014).
- [34] A. L. Burin, *Phys. Rev. B* **91**, 094202 (2015).
- [35] A. L. Burin, *Phys. Rev. B* **92**, 104428 (2015).
- [36] A. Safavi-Naini, M. L. Wall, O. L. Acevedo, A. M. Rey, and R. M. Nandkishore, *Phys. Rev. A* **99**, 033610 (2019).
- [37] S. Schiffer, J. Wang, X.-J. Liu, and H. Hu, *Phys. Rev. A* **100**, 063619 (2019).
- [38] T. Brydges, A. Elben, P. Jurcevic, B. Vermersch, C. Maier, B. P. Lanyon, P. Zoller, R. Blatt, and C. F. Roos, *Science* **364**, 260 (2019).
- [39] M. Dalmonte, S. I. Mirzaei, P. R. Muppalla, D. Marcos, P. Zoller, and G. Kirchmair, *Phys. Rev. B* **92**, 174507 (2015).
- [40] We use the name 'XY-model' following quantum magnetism community. However, it is also often called the XX-model, since the exchange interaction is isotropic in the XY-plane.
- [41] E. Lieb, T. Schultz, and D. Mattis, *Ann. Phys.* **16**, 407 (1961).
- [42] See Appendix at [URL], which includes Refs. [43–49], for the explicit form of the exact conserved charges of the Hamiltonian (1) with  $J_2 = 0$ , and the first quasiserved charge for the case  $J_2/J_1 \ll 1$  and  $h_j = h = \text{const}$ .
- [43] E.V. Gusev, *Theor. Math. Phys.* **53**, 1018 (1982).
- [44] M.P. Grabowski, P. Mathieu, *Ann. Phys.*, **243**, 299 (1995).
- [45] J. Berges, S. Borsanyi, and C. Wetterich, *Phys.Rev.Lett.* **93** 142002, (2004).
- [46] B. Bertini, F. H. L. Essler, S. Groha, and N. J. Robinson, *Phys. Rev. Lett.* **115**, 180601 (2015).
- [47] T. Langen, Th. Gasenzer, and J. Schmiedmayer, *J. Stat. Mech.* **2016**, 064009 (2016).
- [48] T. Mori, T. N. Ikeda, E. Kaminishi, and M. Ueda, *J. Phys. B: At. Mol. Opt. Phys.* **51**, 112001 (2018).
- [49] K. Mallayya, M. Rigol, and W. De Roeck, *Phys. Rev. X* **9**, 021027 (2019).
- [50] D.V. Kurlov, S. Malikis, and V. Gritsev, *arXiv* 2107.04505.
- [51] T. Sugimoto, S. Sota, and T. Tohyama, *Phys. Rev. B* **82**, 035437 (2010).
- [52] K. Nomura and K. Okamoto, *J. Phys. Soc. Jpn.* **62**, 1123 (1993).
- [53] S. Kullback and R. A. Leibler, *Ann. Math. Stat.* **22**, 79 (1951).
- [54] I. M. Khaymovich, V. E. Kravtsov, B. L. Altshuler, and L. B. Ioffe, *Phys. Rev. Research* **2**, 043346 (2020).
- [55] M. Pino, J. Tabanera, and P. Serna, *J. Phys. A: Math. Theor.* **52**, 475101 (2019).
- [56] P. Jordan and E. P. Wigner, *Z. Phys.* **47**, 631 (1928).
- [57] I. Titvinidze and G. Japaridze, *The Eur. Phys. J. B* **32**, 383 (2003).
- [58] J. Carrasquilla, F. Becca, and M. Fabrizio, *Phys. Rev. B* **83**, 245101 (2011).
- [59] F. Crépin, N. Laflorencie, G. Roux, and P. Simon, *Phys. Rev. B* **84**, 054517 (2011).
- [60] V. Khemani, D. N. Sheng, and D. A. Huse, *Phys. Rev. Lett.* **119**, 075702 (2017).
- [61] The determined exponent  $\nu$  indicates the divergent behavior of the characteristic length with  $|\hbar - \hbar_c|^{-\nu}$  and it clearly violates the Harris bound  $\nu \geq 2/d$  (see Refs. [30, 60] for discussions).
- [62] P. S. Kostenetskiy, R. A. Chulkevich and V. I. Kozyrev, *J. Phys.: Conf. Ser.* **1740**, 012050 (2021).

## Appendix

Here in the Appendix we first present the general form of the exact conserved charges of the isotropic XY model in a random magnetic field. We then discuss the quasi-integrability of the isotropic XY model in a homogeneous magnetic field weakly perturbed by the next-nearest neighbor exchange interaction and present the explicit expression for the first non-trivial quasiconserved charge.

Let us consider conserved quantities (charges) for the spin- $\frac{1}{2}$  isotropic XY-model in an inhomogeneous magnetic field. The Hamiltonian is given by

$$H_0 = J_1 \sum_j (S_j^x S_{j+1}^x + S_j^y S_{j+1}^y) + \sum_j h_j S_j^z, \quad (\text{A.1})$$

where  $S_j^\alpha = \sigma_j^\alpha/2$  with  $\alpha \in \{x, y, z\}$ , and  $\sigma_j^\alpha$  are the Pauli matrices acting non-trivially on the  $j$ -th site of the chain,  $J_1$  is the coupling constant for the nearest-neighbor exchange interaction between the spins, and  $h_j$  is the inhomogeneous transverse magnetic field. The Hamiltonian (A.1) is integrable under any boundary conditions and with arbitrary  $h_j$ . It can be diagonalized by the Jordan-Wigner transformation, which reduces Eq. (A.1) to the model of non-interacting spinless fermions [A1].

In the homogeneous case, i.e.  $h_j = h$ , there are two families of conserved charges, which commute with  $H_0$  and each other. Explicitly, they are given by [A2, A3]

$$\begin{aligned} Q_n^{(1)} &= \sum_j (e_{n,j}^{xy} - e_{n,j}^{yx}), \\ Q_n^{(2)} &= J \sum_j (e_{n,j}^{xx} + e_{n,j}^{yy} + e_{n-2,j}^{xx} + e_{n-2,j}^{yy}) - h \sum_j (e_{n-1,j}^{xx} + e_{n-1,j}^{yy}), \end{aligned} \quad (\text{A.2})$$

where by convention  $n \geq 3$  and we denoted

$$e_{n,j}^{\alpha,\beta} = S_j^\alpha S_{j+1}^\beta \cdots S_{j+n-2}^\beta S_{j+n-1}^\alpha, \quad e_{1,j}^{\alpha\alpha} = -S_j^z. \quad (\text{A.3})$$

Note that the combinations  $\sum_j (e_{n,j}^{xx} + e_{n,j}^{yy})$  and  $\sum_j (e_{n,j}^{xy} - e_{n,j}^{yx})$  commute with the total magnetization  $S^z = \sum_j S_j^z$ .

Let us now turn to the case of an inhomogeneous magnetic field, i.e.  $h_j$  is an *arbitrary* function of the lattice site  $j$ . One can show that the Hamiltonian (A.1) commutes with the following conserved charges

$$\mathcal{Q}_n = \sum_j \sum_{k=0}^{n-2} a_j^{(k)} (e_{n-k,j}^{xx} + e_{n-k,j}^{yy}) - \sum_j a_j^{(n-1)} S_j^z, \quad (\text{A.4})$$

given that the coefficients  $a_j^{(m)}$  in Eq. (A.4) satisfy a set of recurrent relations:

$$J (a_{j+1}^{(m)} - a_j^{(m)}) = J (a_j^{(m-2)} - a_{j-1}^{(m-2)}) - a_j^{(m-1)} (h_{j+n-m} - h_j), \quad 0 \leq m \leq n-1, \quad (\text{A.5})$$

where it is implied that for  $l < 0$  we have  $a_j^{(l)} \equiv 0$ . Then, taking  $m = 0$  in Eq. (A.5) we immediately see that  $a_{j+1}^{(0)} = a_j^{(0)}$ , which has only the homogeneous solution  $a_j^{(0)} = a_1^{(0)}$ . The rest of  $n-1$  equations in Eq. (A.5) can be successively solved to determine  $n-1$  remaining coefficients. Thus, we obtain

$$a_j^{(m)} = a_1^{(m)} + \sum_{k=1}^{j-1} \left[ a_k^{(m-2)} - a_{k-1}^{(m-2)} - \frac{1}{J} a_k^{(m-1)} (h_{k+n-m} - h_k) \right], \quad (\text{A.6})$$

which is valid for arbitrary  $h_j$ . It is easy to check that conserved charges  $\mathcal{Q}_n$  in Eq. (A.4) commute with each other. Clearly, for the homogeneous case,  $h_j = h$ , the charges (A.4) coincide with  $Q_n^{(2)}$  in Eq. (A.2), i.e. only one of the families of conserved charges survive in the presence of the inhomogeneous field.

Now we consider the Hamiltonian  $H = H_0 + H_1$ , where  $H_0$  is the integrable part given by Eq. (A.1) with the homogeneous magnetic field,  $h_j = h$ , and  $H_1$  is a perturbation that breaks integrability. We choose the perturbation in the following form:

$$H_1 = J_2 \sum_j (S_j^x S_{j+2}^x + S_j^y S_{j+2}^y), \quad (\text{A.7})$$

which is simply the next-nearest neighbor exchange interaction with the coupling constant  $J_2$ . We assume that the perturbation is weak and one has  $\kappa = J_2/J_1 \ll 1$ . It is believed that in the case of weak integrability-breaking perturbation the model is quasi-integrable. In particular, this implies that it should not thermalize for times as large as  $\tau_{\text{th}} \sim \kappa^{-2}$ , so that the model possesses *approximate* conservation laws that prevent thermalization at shorter times [A4–A8].

Clearly, in the presence of the perturbation (A.7) the charges  $Q_n^{(1,2)}$  from Eq. (A.2) are no longer conserved, since they do not commute with the term  $H_1$ . They are not even quasiconserved, because one has  $\| [H_1, Q_n^{(1,2)}] \| \propto \kappa$ . Therefore, under the evolution with the Hamiltonian  $H = H_0 + H_1$  the operators  $Q_n^{(1,2)}$  change significantly over times much shorter than  $\tau_{\text{th}} \sim \kappa^{-2}$  and can not be responsible for the non-ergodic behaviour in the prethermal phase. Using the procedure discussed in detail in Ref. [A9], one can show that the first non-trivial quasiconserved charge reads

$$\tilde{Q}_3 = Q_3^{(1)} + \kappa \delta Q_3, \quad (\text{A.8})$$

where  $Q_3^{(1)}$  follows from Eq. (A.2) with  $n = 3$  and the correction  $\delta Q_3$  is given by

$$\delta Q_3 = \sum_j S_j^x S_{j+2}^z S_{j+3}^y - \sum_j S_j^y S_{j+2}^z S_{j+3}^x + \sum_j S_j^x S_{j+1}^z S_{j+3}^y - \sum_j S_j^y S_{j+1}^z S_{j+3}^x + \sum_j (\mathbf{S}_j \times \mathbf{S}_{j+1}) \cdot \mathbf{S}_{j+2}, \quad (\text{A.9})$$

where  $\mathbf{S}_j = \{S_j^x, S_j^y, S_j^z\}$  is the vector of spin operators on the  $j$ -th site. One can easily check that  $\tilde{Q}_3$  satisfies the relation

$$\left\| [H_0 + H_1, \tilde{Q}_3] \right\|_F \propto \kappa^2, \quad (\text{A.10})$$

where  $\|X\|_F = \sqrt{\text{tr } X^\dagger X}$  is the Frobenius norm. One can also obtain higher-order quasiconserved charges  $\tilde{Q}_n$ , which commute with the Hamiltonian  $H_0 + H_1$  and each other with the accuracy  $\mathcal{O}(\kappa^2)$ . However, this is beyond the scope of the present paper.

- 
- [A1] E. Lieb, T. Schultz, and D. Mattis, *Ann. Phys.* **16**, 407 (1961).  
[A2] E.V. Gusev, *Theor. Math. Phys.* **53**, 1018 (1982).  
[A3] M.P. Grabowski, P. Mathieu, *Ann. Phys.*, **243**, 299 (1995).  
[A4] J. Berges, S. Borsanyi, and C. Wetterich, *Phys.Rev.Lett.* **93** 142002, (2004).  
[A5] B. Bertini, F. H. L. Essler, S. Groha, and N. J. Robinson, *Phys. Rev. Lett.* **115**, 180601 (2015).  
[A6] T. Langen, Th. Gasenzer, and J. Schmiedmayer, *J. Stat. Mech.* **2016**, 064009 (2016).  
[A7] T. Mori, T. N. Ikeda, E. Kaminishi, and M. Ueda, *J. Phys. B: At. Mol. Opt. Phys.* **51**, 112001 (2018).  
[A8] K. Mallayya, M. Rigol, and W. De Roeck, *Phys. Rev. X* **9**, 021027 (2019).  
[A9] D.V. Kurlov, S. Malikis, and V. Gritsev, *arXiv* 2107.04505.